PHYSICAL REVIEW B VOLUME 18, NUMBER 12 15 DECEMBER 1978

Theory of a solid-state cyclotron maser

A. K. Ganguly and K. R. Chu
Naval Research Laboratory, Washington, D.C. 20375
(Received 24 May 1978)

A theory is developed for the cyclotron-maser interaction between an electron beam and the electromagnetic waves in a cavity formed with a semiconductor having nonparabolic energy bands. The interaction originates from the dependence of the effective mass of the electron (hence cyclotron frequency) on its velocity due to nonparabolic energy-momentum relation. This mechanism is very similar to that for the cyclotron-maser radiation in vacuum tubes where the relativistic variation of mass with velocity is utilized. The linear response of the electron beam to the cavity fields are obtained from the Vlasov equation and the Maxwell's equations, while collisions are treated with an approximate model. Analytical expressions for the beam-wave coupling coefficient, beam energy loss, and the threshold power are derived for the fundamental and higher cyclotron harmonics. The dependence of these quantities on the various parameters such as cavity length, beam position, beam energy, magnetic field, etc., are discussed.

I. INTRODUCTION

The cyclotron-maser radiation[1,2] in an electron beam in vacuum originates from the relativistic variation of electron mass (hence the cyclotron frequency) with velocity. In semiconductors such as InSb, the effective mass of the electrons depend on velocity due to the nonparabolic nature of the energy bands. This property can be utilized to make a solid-state cyclotron maser[3] (CM) in such semiconductors. The maser will operate in the submillimeter range and provide a low-power source of radiation in this frequency range.

As shown by Kane,[4] the energy (W_b) of electrons in the conduction band of InSb is related to momentum ($\vec{p}$) by

$$W_b = \tfrac{1}{2}\left[(E_g^2 + 2E_g p^2/m_0^*)^{1/2} - E_g\right],$$

where m_0^* is the effective mass of the electrons at the bottom of the conduction band and E_g the band gap. From this equation and the relation[5] $\vec{v} = \nabla_{\vec{p}} W_b$, it follows that

$$\vec{v} = \vec{p}/m_0^*(1 + p^2/m_0^{*2}v_g^2)^{1/2} \equiv \vec{p}/m^*,$$

where the parameter m^* is

$$m^* = m_0^*\left(1 + \frac{p^2}{m_0^{*2}v_g^2}\right)^{1/2} = m_0^*\left(1 - \frac{v^2}{v_g^2}\right)^{-1/2} \qquad (1)$$

and $v_g = (E_g/2m_0^*)^{1/2}$. In InSb, $E_g \cong 0.24$ eV, $v_g \cong 1.30 \times 10^6$ m/sec, and $m_0^* \cong 0.014 m_e$, where m_e is the free-electron mass. Because of small values of m_0^* the solid-state cyclotron maser can operate in the submillimeter frequency range with relatively weak magnetic fields of the order of several kilogauss.

If a thin InSb sample at 77 °K is placed in a magnetic field B_0 and electrons are injected in the conduction band at an angle to the magnetic field, the electrons will move in helical trajectories. Initially, the phases of the electrons in the cyclotron orbits are random and no radiation is emitted. But phase bunching can occur due to the dependence of cyclotron frequency $\Omega = eB_0/m^*$ on the electron energy. The electrons that are decelerated in the wave electric field rotate faster and accumulate phase lead while the electrons that are accelerated rotate slower and lag in phase. This results in phase bunching and the electrons radiate coherently at frequency $\omega = s\Omega$, where s is an integer. This mechanism of maser radiation is different from the optically pumped "cyclotron maser" proposed earlier.[6,7]

Theoretical calculations for cyclotron maser in vacuum have been given for two different configurations: (i) the waveguide structure[8] and (ii) the cavity structure.[9] In the first configuration, the electromagnetic wave grows as the result of an instability driven by the electron beam. It corresponds to traveling wave amplification in waveguide structures. In the second model, the electron beam interacts with the constant amplitude standing wave of a cavity structure. It corresponds to beam sustained oscillations in a finite Q cavity. Recently, a theoretical treatment of cyclotron maser in solids was given by Kalmykov *et al.*[3] for the waveguide structure. In their paper, the dispersion relation was derived from the Boltzmann equation in which the collisional integral was disregarded. Conditions for maximum wave growth were obtained from the dispersion relation and the feasibility of a solid-state cyclotron maser was demonstrated.

A major difference between the vacuum cyclotron maser and the solid-state cyclotron maser is the effect of collisions in the latter. Collision

in solids will be a serious obstacle for the phase bunching needed for coherent radiation. The electrons will remain in orbit for a distance close to the mean-free-path length λ_z. For example, in InSb near 77 °K, λ_z is of the order of 10–100 μm.[3,10] For electron velocity of the order of 10^6 m/sec, the Larmour radius $r_L = v_\perp/\Omega$ and the pitch of the spiral $\lambda_c = 2\pi v_z/\Omega$ are of the order of 0.1 and 1 μm, respectively, for a magnetic field $H_0 \cong 5$ kOe. $v_\perp$ and v_z are, respectively, the components of electron velocity perpendicular and parallel to the magnetic field. r_L and λ_c are both much smaller than the mean free path and a large number of turns (λ_z/λ_c) of the electron spiral occurs within λ_z. Thus, electron cyclotron-maser interaction can take place if the interaction length is of the order of λ_z, but the conditions for cyclotron-maser interaction rapidly deteriorate when the interaction length goes much beyond λ_z. In this regard, a solid-state cyclotron maser in the cavity configuration is expected to offer a very significant advantage over the waveguide configuration because the cavity configuration requires a much shorter interaction length. The reason is as follows. In the waveguide case, the beam interacts with an electromagnetic wave that grows from the noise or near-noise level, while in the cavity case the beam interacts with a large amplitude standing wave which has been built up and stored in the cavity. As a result, the interaction is much stronger in the latter case, or in other words, the required interaction length is much shorter in the cavity than in the waveguide in order for the beam to lose the same amount of energy. This is reflected from the fact that in vacuum cyclotron-maser experiments, an oscillator (cavity) is generally shorter than an amplifier (waveguide) by one order of magnitude.

Motivated by the above consideration, here we formulate a detailed solid-state cyclotron-maser theory in cavity. The formalism and the physical expressions to be derived are considerably different from those of the waveguide structure[3] although the basic mechanism is similar. The exact spatial field variation has been incorporated in our calculation and the electron Larmour radius has been kept arbitrary. This allows us to examine interactions at the nonfundamental as well as the fundamental cyclotron frequencies. More importantly, the effect of collisions has also been included in our model. It will be shown that the collisional effect is such a dominant limiting factor in the solid-state cyclotron maser that the short interaction length afforded by the cavity structure could be a decisive advantage over the waveguide structure.

In Sec. II we calculate the linear response of an annular electron beam as it interacts with the cavity modes. The dynamics of the electron beam is determined from the Vlasov equation while the collisions are treated with an approximate model. In Sec. III we calculate the electron beam-cavity mode coupling coefficient, beam energy gain and the threshold beam power necessary to sustain oscillations on the basis of a cold beam assumption. We also show the dependence of these quantities on the various parameters such as beam position, beam energy, cavity length, and the magnetic field. In Sec. IV we discuss the results from our theory and suggest some experimental configurations to observe the oscillations.

II. MODEL AND FORMALISM

Figure 1 shows the configuration of the electron cyclotron-maser system under consideration. An annular beam of electrons is guided by the magnetic field B_0 along helical trajectories inside a circular-cross-section InSb cavity (radius R and length $L < \lambda_z$). The electrons are injected at an angle to the magnetic field such that a major part of their kinetic energy is in the form of transverse gyromotion and the rest in the form of axial motion. The axis of the trajectories is along the cavity (z axis). The cyclotron orbits may or may not encircle the axis of the cavity, depending on how the beam is formed. In Fig. 1 the second type

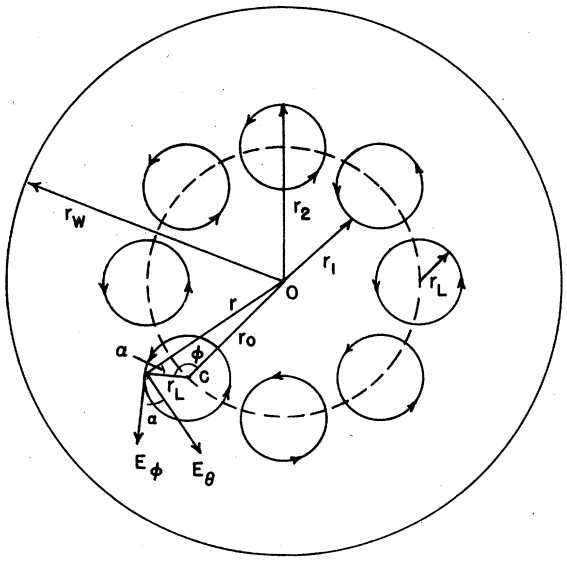

FIG. 1. End view of the electron cyclotron maser. Guiding centers are uniformly distributed on a circle of radius r_0. The point 0 is the axis of symmetry. The circle of radius r_L is an arbitrarily chosen electron orbit and c is the guiding center of this electron. E_θ is the electric field of the cavity and E_φ is the component of E_θ tangential to the electron orbit.

of orbits is shown. We make the following simplifying assumptions to obtain the linear response of the electron beam: (i) the beam is sufficiently weak so that its self-electro-static and magnetic fields are small compared with the cavity fields; (ii) the cavity fields are of first order with respect to the applied magnetic field B_0 and the perturbed electron distribution $f^{(1)}$ caused by these fields is of first order with respect to the initial distribution function f_0; (iii) the distribution function and the cavity fields are independent of the azimuthal angle θ; and (iv) the electron collision frequency is much smaller than the electron cyclotron frequency.

The cavity modes may be classified as TE or TM modes. Cyclotron maser interaction is much stronger for TE modes than the TM modes.[1] Thus, we consider only TE modes and in accordance with assumptions (i) and (iii) restrict our attention to TE_{0nm} modes given by

$$E_\theta^{(1)} = E_{\theta_0} J_1(k_n r) \sin k_z z \cos\omega t , \tag{2a}$$

$$B_r^{(1)} = (k_z/\omega) E_{\theta_0} J_1 + (k_n r) \cos k_z z \sin\omega t , \tag{2b}$$

$$B_z^{(1)} = -(k_n/\omega) E_{\theta_0} J_0(k_n r) \sin k_z z \cos\omega t , \tag{2c}$$

where

$$k_z = m\pi/L , \tag{3a}$$

$$k_n = x_n/R , \tag{3b}$$

x_n being the nth nonvanishing root of $J_1(x)$ and the wave frequency

$$\omega = (k_z^2 + k_n^2)^{1/2}/(\mu\epsilon)^{1/2} . \tag{3c}$$

$J_p(x)$ is the Bessel function of order J_p. μ and ϵ denote, respectively, the permeability and the dielectric constant of the medium; $c = (\mu_0\epsilon_0)^{-1/2}$ is the velocity of light in vacuum. We assume that $\mu = \mu_0$. The subscript (1) refers to the first-order quantities. We use MKS units throughout the paper.

The electron distribution function f is determined by the equation

$$\frac{\partial f}{\partial t} + \frac{\vec{p}}{m^*} \cdot \nabla f - e\left(\vec{E} + \frac{\vec{p}\times\vec{B}}{m^*}\right) \cdot \nabla_{\vec{p}} f = \left(\frac{\partial f}{\partial t}\right)_{\text{coll}} , \tag{4}$$

where $(\partial f/\partial t)_{\text{coll}}$ is a collision term whose form will be specified later.

On the basis of the two different time scales assumed [assumption (iv)], we may separate the distribution function f into a slowly varying component f_s representing the collisional relaxation of the zero-order distribution function and a rapidly varying component $f^{(1)}$ representing the perturbation caused by the wave field. A characteristic of the cyclotron maser system is that the cavity structure, rather than the electron medium, determines the properties of the wave (spatial profile and dispersion relation, etc.). Thus, only those electrons which interact resonantly with the wave are of importance while the effects of non-resonant electrons can be neglected. As will be determined in Sec. III, resonant electrons occupy a very narrow region in the velocity space. Hence the initial distribution function of interest to the problem would be one in which all the electrons fall in the resonant region. Further it is reasonable to assume that if an electron suffers a collision in its path, it will be scattered off the resonant region and consequently its dynamics will no longer be of interest. Thus we may approximately write f_s as

$$f_s(\vec{r}, \vec{p}, t) = f_0(\vec{r}, \vec{p}) \exp[-\nu(t - t_0)] , \tag{5}$$

where t_0 is the time an electron first enters the cavity, $\nu = v_z/\lambda_z$ is the collision frequency, and $f_0(\vec{r}, \vec{p})$ is any function which satisfied the zero-order Vlasov equation[11] in the absence of collisions. Since the cavity length $L < \lambda_z$, very few collisions occur and the approximate form for f_s in Eq. (5) should be adequate for our purpose.

On linearizing Eq. (4) according to the ordering scheme in assumption (ii), we obtain the following equation for the perturbed distribution function $f^{(1)}$:

$$\left(\frac{\partial}{\partial t} + \frac{\vec{p}}{m^*} \cdot \nabla - \frac{e}{m^*}(\vec{p}\times\vec{B}_0) \cdot \nabla_{\vec{p}}\right) f^{(1)}(\vec{r}, \vec{p}, t)$$
$$= -\nu f^{(1)}(\vec{r}, \vec{p}, t) + e\left(\vec{E}^{(1)}(\vec{r}, t) + \frac{\vec{p}\times\vec{B}^{(1)}(\vec{r}, t)}{m^*}\right) \cdot \nabla_{\vec{p}} f_s(\vec{r}, \vec{p}, t) , \tag{6}$$

where $m^* = \gamma m_0^*$ with

$$\gamma = [1 - (v_\perp^2 + v_z^2)/v_z^2]^{-1/2} . \tag{7}$$

Note that in Eq. (7), the Bhatnagar-Gross-Krook (BGK) model[12] of collisions has been assumed. Equation (6) may be solved by the method of characteristics, namely, by intergrating it along unperturbed trajectories of the electrons. Equation (6) thus reduces to

$$f^{(1)}(\vec{r}, \vec{p}, t) = e \int_{t_0}^{t} dt' \exp[\nu(t' - t)] \times \left(\vec{E}^{(1)}(\vec{r}', t') + \frac{\vec{p}'\times\vec{B}^{(1)}(\vec{r}', t')}{m^*}\right) \cdot \nabla_{\vec{p}'} f_s(\vec{r}', \vec{p}', t') , \tag{8}$$

where the t' integration is along the unperturbed orbits. The primed quantities $\vec{r}'$ and $\vec{p}'$ are treated as functions of t' while $\vec{r}$ and $\vec{p}$ are, respectively the values of $\vec{r}'$ and $\vec{p}'$ at $t' = t$. The lower limit of the integration t_0 is given by $t_0 = t - z/v_z$, i.e.,

the time an electron at axial position z and time t first enters the cavity. Substituting Eq. (5) in Eq. (8) and using the relation $t_0 = t - z/v_z$, we obtain

$$f^{(1)}(\vec{r},\vec{p},t) = \exp\left(\frac{-z}{\lambda_z}\right)\cdot\int_{t-z/v_z}^{t} dt'\, e\left(\vec{E}^{(1)}(\vec{r}',t') + \frac{\vec{p}'\times\vec{B}^{(1)}(\vec{r}',t')}{m^*}\right)\cdot\nabla_{\vec{p}'} f_0(\vec{r}',\vec{p}') \ . \tag{9}$$

In the absence of collision $f^{(1)}$ is given by the integral alone on the right-hand side of Eq. (9). Collisions reduce $f^{(1)}$ by the factor $\exp(-z/\lambda_z)$.

The methods for evaluating the integral in Eq. (9) are standard[11] and the result may be written in the form

$$f^{(1)} = f_+^{(1)} + f_-^{(1)} \ , \tag{10}$$

where

$$f_+^{(1)} = \mathrm{Im}\left\{\frac{eE_{\theta_0}}{2\omega} e^{i(k_z z-\omega t)-z/\lambda_z}\left[\left(\omega - \frac{k_z p_z}{m^*}\right)\frac{\partial f_0}{\partial p_\perp} + \frac{k_z p_\perp}{m^*}\frac{\partial f_0}{\partial p_z}\right] \times \sum_{s=-\infty}^{+\infty}\sum_{s'=-\infty}^{+\infty} i^{s'-1}\frac{J_{s'}(k_n r)G_{ss'}(k_n r_L)Xe^{-is'(\varphi-\theta)}}{\omega - k_z p_z/m^* - s\Omega}\right\} , \tag{11}$$

with

$$\Omega = \frac{eB_0}{m^*} = \frac{\Omega_0}{\gamma} \ , \quad r_L = \frac{p_\perp}{m_0^*\Omega_0} \ , \quad X = 1 - \exp\left(\frac{i(\omega - k_z v_z - s\Omega)z}{v_z}\right) , \quad G_{ss'}(x) = J_{s+s'}(x)\frac{dJ_s(x)}{dx} \ . \tag{12}$$

In Eq. (11), $\mathrm{Im}\{A\}$ indicates the imaginary part of A. φ and θ are, respectively, the polar angles of the momentum and position vectors. $p_\perp$ and p_z denote the components of momentum $\vec{p} = m^*\vec{v}$, perpendicular and parallel, respectively, to the external magnetic field. $f_-^{(1)}$ is given by Eq. (11) with ω replaced by $-\omega$. In obtaining Eq. (11) we have used the following relation.[13]:

$$e^{is\theta_1}J_s(x_1) = \sum_{s'=-\infty}^{+\infty} J_{s+s'}(x_2)J_{s'}(x_3)e^{is'\theta_2} \ ,$$

where x_1, x_2, x_3, θ_1, and θ_2 are related through the triangle shown in Fig. 2.

The perturbed azimuthal current $J_\theta^{(1)}$ is given by

$$J_\theta^{(1)} = -e\int f^{(1)}v_\theta\, d^3p = -e\int_0^\infty p_\perp dp_\perp \int_{-\infty}^{+\infty} dp_z \int_0^{2\pi} d\hat{\varphi}\, f^{(1)}v_\perp \sin\hat{\varphi} \ , \tag{13}$$

where $\hat{\varphi} = \varphi - \theta$. From Eqs. (10)–(13), we obtain, after integration by parts over $p_\perp$ and p_z,

$$J_\theta^{(1)} = J_{\theta+}^{(1)} + J_{\theta-}^{(1)} \ , \tag{14}$$

where

$$J_{\theta+}^{(1)} = \mathrm{Im}\left[\frac{e^2E_{\theta_0}}{4m_0^*\omega} e^{i(k_z z-\omega t)-z/\lambda_z}\sum_{s=-\infty}^{+\infty}\sum_{s'=-\infty}^{+\infty} J_{s'}(k_n r) \times \int_0^\infty p_\perp dp_\perp \int_{-\infty}^{+\infty} dp_z \int_0^{2\pi} d\hat{\varphi}\, f_0 i^{s'}(e^{-i(s'-1)\hat{\varphi}} - e^{-i(s'+1)\hat{\varphi}}) \times\left(\frac{G_{ss'}(k_n r_L)p_\perp^2(\omega^2 - k_z^2v_z^2)X}{\gamma^3 m_0^{*2}v_z^2\eta^2} - \frac{(\omega - k_z v_z)X[2G_{ss'}(k_n r_L) + k_n r_L G'_{ss'}(k_n r_L)]}{\gamma\eta} + \frac{iz(1-X)(\omega^2 - k_z^2v_z^2 - k_z v_z^2\eta/v_z)p_\perp^2}{\gamma^2 m_0^* v_z^2 p_z\eta}\right)\right] , \tag{15}$$

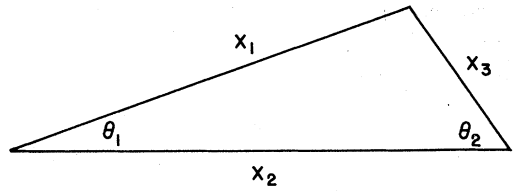

FIG. 2. Geometrical relations of the variables used in the Bessel function identity.

with $\eta=\omega-k_z v_z-s\Omega$ and $G'_{ss'}(x)=dG_{ss'}(x)/dx$. $J_{\theta-}^{(1)}$ is given by Eq. (15) with ω replaced by $-\omega$.

Equation (14) gives the perturbed current for a general distribution function f_0. In the following we specialize to a particular distribution function which is considered to be the most ideal for cyclotron-maser operation.[9] It is constructed from the constants of motion of the system (in the absence of collision): $p_\perp$, p_z, and $L_\theta=\gamma m^* v_\perp r\sin\hat{\varphi}-\frac{1}{2}eB_0r^2$. We assume that[9]

$$f_0=k\delta\left(r_L^2-\frac{2L_\theta}{eB_0}-r_0^2\right)\frac{\delta(p_\perp-p_\perp^0)\delta(p_z-p_z^0)}{2\pi p_\perp}, \quad (16)$$

which represents a cold monoenergetic beam moving along helical trajectories with guiding centers distributed uniformly on a cylinder of radius r_0. The constant k is determined by the normalization condition

$$\int f_0 2\pi r\,dr\,d^3p=N, \quad (17)$$

where N is the line density of the electrons (i.e., number of electrons per unit length). Equation (16) may be written

$$f_0=\frac{N\delta(p_z-p_z^0)\delta(p_\perp-p_\perp^0)}{2\pi^2 p_\perp[(r^2-r_1^2)(r_2^2-r^2)]^{1/2}}\times[\delta(\hat{\varphi}-\hat{\varphi}_0)+\delta(\hat{\varphi}-\pi+\hat{\varphi}_0)]\times\theta(r-r_1)\theta(r_2-r), \quad (18)$$

where

$$\hat{\varphi}_0=\sin^{-1}[(r^2+r_L^2-r_0^2)/2rr_L];$$

$$\theta(x)=\begin{cases}1 & \text{for } x\geq 0,\\ 0 & \text{for } x<0;\end{cases}$$

$$r_1=|r_0-r_L| \text{ and } r_2=|r_0+r_L|.$$

The idealized distribution function in Eq. (18) leads to results which can be physically interpreted and provides valuable information for the operation of the solid-state gyrotron.

III. BEAM POWER GAIN AND THRESHOLD POWER

The time average power gain for all the electrons in the cavity is given by

$$P=\omega\int_0^{2\pi/\omega}dt\int_0^R dr\int_0^L J_\theta^{(1)}E_\theta^{(1)}dz. \quad (19)$$

We introduce the following notation:

$$\begin{aligned}&\beta_z=v_z/c,\\ &\beta_{\perp0}=p_\perp^0/\gamma_0 m_0^* c=v_{\perp0}/c,\\ &\beta_{z0}=p_z^0/\gamma_0 m_0^* c=v_{z0}/c,\\ &\gamma_0=[1-(\beta_{\perp0}^2+\beta_{z0}^2)/\beta_z^2]^{-1/2},\\ &\tau=L/v_{z0},\\ &\Delta_0=\omega^2\tau^2-k_z^2L^2\beta_z^2/\beta_z^2,\\ &\Delta=\omega\tau-k_zL-s\Omega_0\tau/\gamma_0,\\ &\Delta'=\omega\tau+k_zL-s\Omega_0\tau/\gamma_0.\end{aligned} \quad (20)$$

τ is the transit time of the electrons in the cavity and $\nu\tau=L/\lambda_z$. From Eqs. (2a), (14), (15), and (18)–(20), we have

$$P=\frac{NLe^2E_{\theta0}^2}{8m_0^*\gamma_0\omega}\sum_{s=-\infty}^{+\infty}(\alpha_{s1}+\alpha_{s2}-\alpha_{s3}-\alpha_{s4}), \quad (21)$$

where

$$\alpha_{s1}=-\frac{H_s(k_nr_0,k_nr_L)\beta_{\perp0}^2}{\Delta\beta_z^2}\times\left[\Delta_0\left(N(\Delta)+\frac{M(\Delta)}{\Delta}\right)-\frac{k_zL\Delta\beta_z^2}{\beta_z^2}N(\Delta)\right]+\frac{Q_s(k_nr_0,k_nr_L)}{\Delta}(\omega\tau-k_zL)M(\Delta), \quad (22)$$

$$\alpha_{s2}=\frac{H_s(k_nr_0,k_nr_L)\beta_{\perp0}^2}{\Delta\beta_z^2}\times\left[\Delta_0\left(N(\Delta')+\frac{M(\Delta')}{\Delta}-\frac{\Gamma}{\Delta}\right)-\frac{k_zL\Delta\beta_z^2N(\Delta')}{\beta_z^2}\right]-\frac{Q_s(k_nr_0,k_nr_L)}{\Delta}(\omega\tau-k_zL)[M(\Delta')-\Gamma], \quad (23)$$

with

$$M(x)=\frac{x(1-e^{-\nu\tau}\cos x)-\nu\tau e^{-\nu\tau}\sin x}{x^2+\nu^2\tau^2}, \quad (24)$$

$$N(x)=\mathrm{Re}\left(\frac{1-e^{-\nu\tau}e^{ix}}{(x+i\nu\tau)^2}+\frac{ie^{-\nu\tau}e^{ix}}{x+i\nu\tau}\right), \quad (25)$$

$$\Gamma=2k_zL(1-e^{-\nu\tau})/(4k_z^2L^2+\nu^2\tau^2). \quad (26)$$

The quantities α_{s3} and α_{s4} are, respectively, obtained from α_{s1} and α_{s2} with the following replacements:

$$\omega \to -\omega, \ \Delta \to -\Delta' \ \text{and} \ \Delta' \to -\Delta \ .$$

The functions $H_s(a_0, a_L)$ and $Q_s(a_0, a_L)$ are defined by

$$H_s = J_s'(a_L) I_s(a_0, a_L) \ , \tag{27}$$

$$Q_s = 2H_s(a_0, a_L) + a_L J_s''(a_L) I_s(a_0, a_L) + \tfrac{1}{2} a_L J_s'(a_L)[I_{s-1}(a_0, a_L) - I_{s+1}(a_0, a_L)] \ , \tag{28}$$

where

$$I_s(a_0, a_L) = -\frac{2}{\pi} \int_{a_1}^{a_2} da J_1(a) a \times \sin\hat{\varphi}[(a^2 - a_1^2)(a_2^2 - a^2)]^{-1/2} \times \sum_{s'=-\infty}^{\infty} J_{s+s'}(a_L) J_{s'}(a) \cos s' \left(\frac{\pi}{2} - \hat{\varphi}\right) \tag{29}$$

and

$$a_1 \equiv |a_0 - a_L| , \quad a_2 \equiv |a_0 + a_L| ,$$

and

$$\varphi = \sin^{-1}[(a^2 + a_L^2 - a_0^2)/2aa_L] \ .$$

The integral series in Eq. (29) is evaluated in Appendix A and found to be[9]

$$I_s(a_0, a_L) = J_s^2(a_0) J_s'(a_L) \ . \tag{30}$$

Equation (21) contains a summation over all harmonics of the cyclotron frequency. As we shall see later, radiation is favored at a particular cyclotron frequency near the synchronous condition

$$\omega - k_z v_{z0} - s\Omega_0/\gamma_0 = 0 \ .$$

Hence in Eq. (21) we keep only one term. We are mostly interested in the fundamental cyclotron frequency. In later calculations parameters are chosen such that $s = 1$ term dominates. In the case $\nu = 0$, the quantities α assume the form

$$\alpha_1 = -H_s \left(\frac{\beta_{\perp 0}}{\beta_z}\right)^2 \left\{ \left(\omega^2\tau^2 - \frac{k_z^2 L^2 \beta_z^2}{\beta_z^2}\right) \times \left[4 \sin^2\left(\frac{\Delta}{2}\right) - \Delta \sin\Delta\right] + k_z L \left(\frac{\beta_z^2}{\beta_z^2}\right) \Delta \left[\Delta \sin\Delta - 2 \sin^2\left(\frac{\Delta}{2}\right)\right] \right\} / \Delta^3 + \frac{2Q_s(\omega\tau - k_z L) \sin^2(\frac{1}{2}\Delta)}{\Delta^2} \ , \tag{31}$$

$$\alpha_2 = H_s \left(\frac{\beta_{\perp 0}}{\beta_z}\right)^2 \left\{ \left(\omega^2\tau^2 - \frac{k_z^2 L^2 \beta_z^2}{\beta_z^2}\right) \left[2\left(1 + \frac{\Delta}{\Delta'}\right) \sin^2\left(\frac{\Delta'}{2}\right) - \Delta \sin\Delta'\right] + k_z L \left(\frac{\beta_z^2}{\beta_z^2}\right) \Delta \left[\Delta \sin\Delta' - 2\left(\frac{\Delta}{\Delta'}\right) \sin^2\left(\frac{\Delta'}{2}\right)\right] \right\} \Big/ (\Delta^2 \Delta') - \frac{2Q_s(\omega\tau - k_z L) \sin^2(\frac{1}{2}\Delta')}{(\Delta\Delta')} \ . \tag{32}$$

The other two quantities α_3 and α_4 are obtained by the replacements

$$\omega \to -\omega, \quad \Delta \to -\Delta', \quad \text{and} \ \Delta' \to -\Delta$$

in the expressions for α_1 and α_2, respectively.

In Eq. (10), $f_+^{(1)}$ and $f_-^{(1)}$ may be regarded as perturbation in the electron distribution function due to the forward- and backward-traveling waves which make up the standing cavity modes. In Eq. (21), the terms α_{s1} and α_{s2} arise from interaction of $f_+^{(1)}$ with the forward- and the backward-traveling waves. Similarly, α_{s3} and α_{s4} terms are due to the interaction of $f_-^{(1)}$ with the two waves.

In the expression for α's, the first term (proportional to $H_s \beta_{\perp 0}^2$) arise from the transverse motion of the electrons and the second term [proportional to $(\omega\tau - k_z L) Q_s$] is due to wave-induced oscillations. The first term is much larger than the second term unless $\beta_{\perp 0}$ is too low. Hence the coupling between the electron beam and the cavity modes is essentially proportional to $H_s(k_n r_0, k_n r_L)$. The first term may be positive (beam-power gain) or negative (beam-power loss) depending on the phase factor Δ. It is shown in Appendix B that E_φ, the amplitude of the component of the cavity electric field tangential to the electron cyclotron orbit (see Fig. 1) may be written

$$E_\varphi = -AE_{\theta 0} \sum_{s=0}^{+\infty} H_s^{1/2}(k_n r_0, k_n r_L) \cos s\varphi \ ,$$

where $A=1$ for $s=0$ and $A=2$ for $s\neq 0$. Thus $E_{\theta_0}H_s^{1/2}$ may be interpreted as the sth harmonic component of the effective electric field in the direction of the electron velocity and the beam-power gain is proportional to H_s.

In the expression for P, the guiding center position r_0 enters through $H_s(k_n r_0, k_n r_L)$. Hence P can be maximized by maximizing H_s with respect to r_0 for each combination of n and s. Numerical computation shows that the optimum value of r_0 is $0.48R$ for $n=s=1$. This value of r_0 will be used in later calculations.

The total stored energy (W) in the cavity is given by

$$W=\tfrac{1}{4}\pi R^2 L\epsilon J_0^2(k_n R)E_{\theta_0}^2 . \tag{33}$$

Let us define a dimensionless quantity F,

$$F=P\tau/W \tag{34}$$

as the ratio of the total beam-energy gain during one transit time to the total stored field energy. From Eqs. (21), (33), and (34), we get

$$F=\omega_p^2\tau\alpha/2\gamma_0 J_0^2(x_n)\omega , \tag{35}$$

where $\omega_p=(Ne^2/\pi R^2\epsilon m_0^*)^{1/2}$ and $\alpha=(\alpha_1+\alpha_2-\alpha_3-\alpha_4)$.

The quantity F may be positive or negative depending on the value of the phase factor Δ. The beam generates electromagnetic radiation in the range of Δ for which F is negative.

An actual cavity has a finite Q due to dielectric losses or loading or wall resistivity or end faces not being perfectly reflecting and energy is lost from the cavity at the rate

$$P_{\text{out}}=\omega W/Q . \tag{36}$$

The electron beam generates energy at the rate

$$P_{\text{in}}=-FW/\tau . \tag{37}$$

Thus the threshold condition for cavity oscillations is given by

$$-FQ\geq\omega\tau . \tag{38}$$

The energy of the electrons in the conduction band of the crystal may be written

$$W_b=(\gamma_0-1)m_0^*\beta_g^2c^2 , \tag{39}$$

and the electron beam power inside the crystal is

$$P_b=N(\gamma_0-1)m_0^*\beta_g^2c^2v_{z0} . \tag{40}$$

From Eqs. (35), (38), and (40), we find that

$$P_b\geq P_b^{\text{th}} , \tag{41}$$

where the threshold beam power P_b^{th} is given by

$$P_b^{\text{th}}=-\left(\frac{\omega R}{c}\right)^2\frac{\gamma_0(\gamma_0-1)\beta_g^2\beta_{z0}J_0^2(x_n)}{\alpha Q}\times\frac{4\pi\epsilon m_0^{*2}c^5}{2e^2} . \tag{42}$$

The result for cyclotron maser in vacuum is recovered by setting $\epsilon=\epsilon_0$, $\beta_g=1$, and $m_0^*=m_e$ in Eq. (42). Since $\beta_g=4.3\times10^{-3}$ and $m_0^*=0.014m_e$ in InSb at 77 °K, the threshold beam power for the solid-state cyclotron maser is many orders of magnitude lower than that of the vacuum case. Numerical examples for F and P_b^{th} are given in Sec. IV.

IV. NUMERICAL RESULTS AND DISCUSSION

The quantity F [Eq. (35)] and the product QP_b^{th} [Eq. (42)] depend on the parameters s, n, m, R, r_0, λ_g, γ_0, $v_{\perp0}/v_{z0}$, and Ω. For numerical examples we consider only the fundamental mode numbers, i.e., $s=m=n=1$. In this case $x_n=k_nR=3.832$, $k_gL=\pi$, and $\Delta'=\Delta+2\pi$. As shown earlier r_0 should be $0.48R$ to maximize $H_s(x_nr_0/R, x_nr_L/R)$. From Eqs. (35) and (42) it can be seen that the radius of the cavity R may be scaled out by normalizing length to R and frequency to c/R. Wave vector, time, and velocity are correspondingly normalized. The natural dimensionless quantities γ_0, β, Δ, $\omega\tau$, k_gL, H_s, and Q_s remain unchanged. For a given $\bar{L}=L/R$, $\bar{\omega}=c\omega/R$ is fixed by Eq. (3c). F and QP_b^{th} are obtained numerically for various values of the parameters $\bar{L}$, γ_0, $\beta_{\perp0}/\beta_{z0}$, and $\bar{\Omega}=c\Omega/R$ (i.e., Δ).

Figures 3(a) and 3(b) show typical plots of F as a function of Δ. F becomes negative for Δ in the range $-0.9\pi<\Delta<2\pi$. The lower limit does not change with $\bar{L}$ and shows slight changes only with γ_0, and $\beta_{\perp0}/\beta_{z0}$. The maximum negative gain $-F_m$ increases with increase in γ_0, $\beta_{\perp0}/\beta_{z0}$, and $\bar{L}$. The magnitude of F decreases with $\nu\tau$ as expected. α_1, α_2, α_3, and α_4 are also plotted as function of Δ in Fig. 3. α_4 differs only slightly from α_2. In the traveling-wave structure, the gain is determined by the term α_1. In this case gain is negative only[3,8] for $\Delta>0$. The phase factor Δ_m corresponding to $-F_m$ lies near $+0.1\pi$. Δ_m shifts slightly towards lower values with increase in $\bar{L}$, γ_0, and $\beta_{\perp0}/\beta_{z0}$.

In Fig. 4, QP_b^{th} is plotted as a function of the electron energy in the crystal $W_b=(\gamma_0-1)m_0^*c^2\beta_g^2$ for cyclotron frequency $\bar{\Omega}$ corresponding to Δ_m. Data are shown for $\beta_{\perp0}/\beta_{z0}=1.5$ and different values of $\bar{L}$ and $\nu\tau=L/\lambda_g$. The threshold power increases with decrease in $\bar{L}$ and increase in $\nu\tau$. QP_b^{th} is of the order of 10^{-3} W for electron energies $\sim10^{-3}$ eV. For $\bar{L}=0.05$ and $\nu\tau=0.5$, $QP_b^{\text{th}}=1.8$ mW at $W_b=13.2$ meV. Assuming $Q\cong100$,

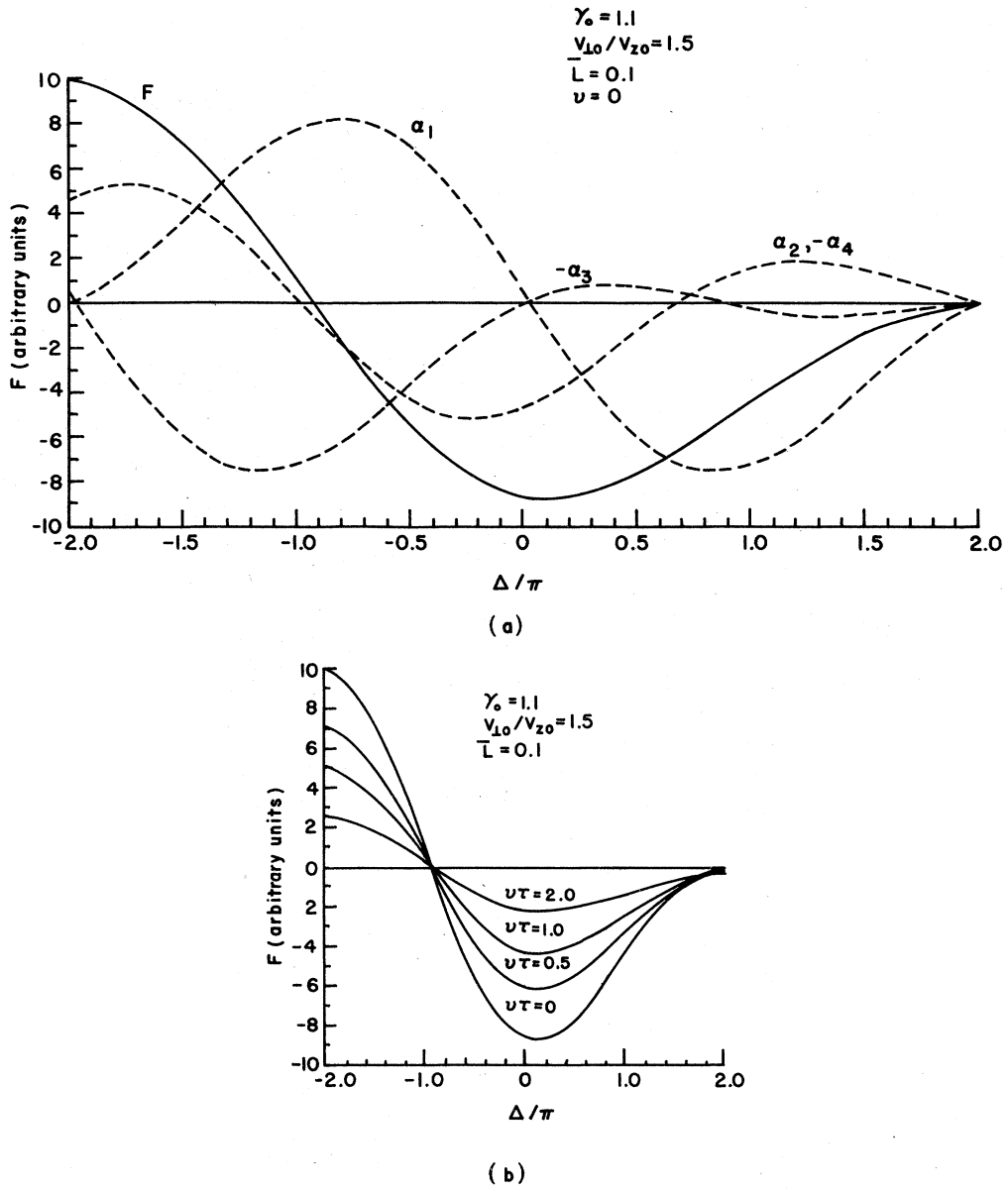

FIG. 3. (a) F (solid curve) vs Δ for $n=s=m=1$, $\bar{r}_0=0.48$, $\bar{L}=0.1$, $\gamma_0=1.1$, $\beta_{\perp 0}/\beta_{z0}=1.5$, and $\nu\tau=0$. The dashed curves marked α_1, α_2, α_3, and α_4 are plots of the four components of F as function of Δ. Dielectric constant $\epsilon=17.7\epsilon_0$. (b) F as a function of Δ for four different values of $\nu\tau$ with other parameters the same as in (a).

$P_b^{\rm th}\cong 18$ μW. As the length of the cavity is decreased to reduce the effect of collisions, the lowest eigenfrequency increases. For mean free path $\lambda_z\cong 100$ μm and $\bar{L}=0.05$, the operating frequencies at $\nu\tau=1.0$ and 0.5 are, respectively, 367 and 734 GHz. The corresponding cyclotron frequencies Ω for maximum beam energy loss are 357.4 ($H_0=1787$ Oe) and 715 GHz ($H_0=3575$ Oe).

We make some suggestions for possible experiments to observe solid-state cyclotron-maser radiation. The cavity might be in the form of a disk with polished ends and metallized edges. The thickness of the disk should be less than a mean free path of the electrons. The cavity is placed in a uniform magnetic field. One end face of the disk is bombarded by an electron beam at an angle to the field such that the electrons get into the conduction band with appropriate transverse and axi-

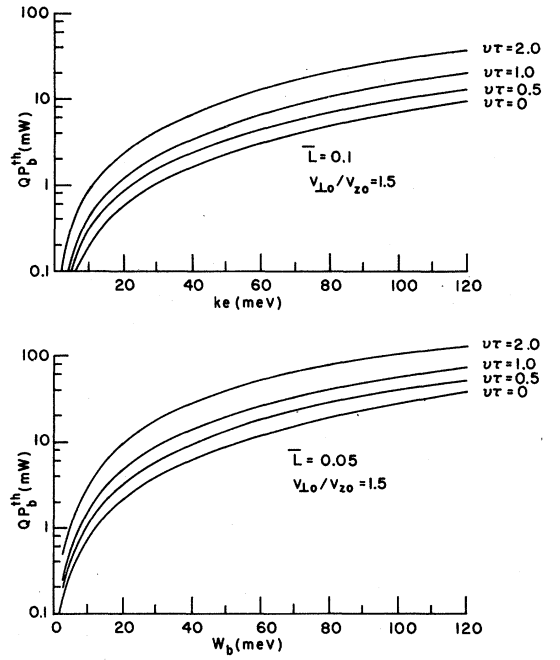

FIG. 4. P_b^{th}, the threshold beam power, as a function of the beam kinetic energy W_b for $n=s=m=1$, $\bar{r}_0=0.48$, $\beta_{\perp 0}/\beta_{z0}=1.5$, and (a) $\bar{L}=0.1$, (b) $\bar{L}=0.05$. The magnetic field is chosen so as to maximize the beam energy loss. Curves are shown for three different values of $\nu\tau$.

al velocities. Another possibility is to use the structure under forward bias condition with a doping profile similar to that of a Read diode[14] (n^+pip^+), such that there is a very narrow accelerating region of high dc electric field and a larger intrinsic region where the dc electric field is negligible. Cyclotron-maser radiation takes place in this region.

V. CONCLUSION

In this paper we propose the operation of a solid-state cyclotron maser in the cavity configuration and demonstrate its feasibility with a theoretical analysis. We have derived analytical expressions for both the electromagnetic power gain and the threshold beam power. The dependence of these two quantities on the various parameters such as the length and radius of the cavity, electron mean free path, the magnetic field, initial electron beam energy, radial and axial eigenmode number, cyclotron mode, etc., has been shown. In order to minimize the effects of collision, the cavity length should be less than a mean free path of electrons. This sets a lower limit to the frequency that can be used. It is seen from Eqs. (35) and (40) that a better performance is obtained with a material having large mean free path λ_g, small band gap, i.e., v_g, and small effective mass m_0^*. The cavity length can be increased and the frequency of operation lowered if λ_g is larger. Since the cyclotron frequency is proportional to B_0/m_0^*, smaller magnetic fields are required for materials with smaller m_0^*. Furthermore, P_b^{th} decreases as m_0^*. A smaller value of v_g is also desirable because P_b^{th} is lowered and electron velocity needed to obtain a given value of γ_0 is also reduced. Our results are based on a linear theory. A nonlinear theory is necessary to calculate the efficiency and the saturation power level of the system. This will be the subject of a future investigation.

ACKNOWLEDGMENT

The authors are indebted to Dr. K. L. Davis for many helpful discussions.

APPENDIX A

The integral series $I_s(a_0, a_L)$ appearing in Eqs. (27) and (28) is defined as

$$I_s(a_0,a_L)\equiv\frac{-2}{\pi}\int_{a_1}^{a_2} da\,\sin\phi_0 J_1(a)a \times[(a^2-a_1^2)(a_2^2-a^2)]^{-1/2} \times\sum_{s'=-\infty}^{\infty} J_{s+s'}(a_L)J_{s'}(a) \times\cos s'\left(\frac{\pi}{2}-\phi_0\right), \tag{A1}$$

where

$$a_1=|a_0-a_L|,\quad a_2=a_0+a_L,$$

and

$$\phi_0=\sin^{-1}[(a^2+a_L^2-a_0^2)/2aa_L]\,. \tag{A2}$$

Inserting Eq. (A2) into Eq. (A1) and using the Bessel-function identity

$$J_s(w)\cos s\Psi=\sum_{s'=-\infty}^{\infty} J_{s+s'}(u)J_{s'}(v)\cos s'a, \tag{A3}$$

where $w=(u^2+v^2-2uv\cos a)^{1/2}$ and $\Psi=\cos^{-1}[(u-v\cos a)/w]$, we reduce Eq. (A1) to (after some algebra)

$$I_s(a_0,a_L)=-\frac{J_s(a_0)}{\pi} \times\int_{a_1}^{a_2} da\,\frac{J_1(a)(a^2+a_L^2-a_0^2)^2}{a_L[(a^2-a_1^2)(a_2^2-a^2)]^{1/2}} \times\cos\left(s\cos^{-1}\frac{a_L^2+a_0^2-a^2}{2a_0a_L}\right). \tag{A4}$$

To carry out the integration in Eq. (A4), we replace the variable of integration a with x, where x is defined through the equation

$$a=(a_0^2+a_L^2-2a_0a_L\cos x)^{1/2}\ .$$

Again after some algebra, we obtain

$$\begin{aligned} I_s(a_0,a_L) &= -\frac{J_s(a_0)}{\pi} \\ &\times\int_0^{\pi} dx\,\frac{J_1[(a_0^2+a_L^2-2a_0a_L\cos x)^{1/2}]}{(a_0^2+a_L^2-2a_0a_L\cos x)^{1/2}} \\ &\times(a_L-a_0\cos x)\cos sx \\ &=\frac{1}{\pi}J_s(a_0)\frac{d}{da_L} \\ &\times\int_0^{\pi} dx\,J_0[(a_0^2+a_L^2-2a_0a_L\cos x)^{1/2}]\cos sx\ , \end{aligned} \tag{A5}$$

Using tabulated integral *formula*,[13] we obtain

$$I_s(a_0,a_L)=J_s^2(a_0)J_s'(a_L)\ . \tag{A6}$$

APPENDIX B

The component of the cavity electric field tangential to the electron cyclotron orbit is

$$E_\phi=E_\theta\cos\alpha=E_{\theta 0}J_1(k_nr)\cos\alpha\ , \tag{B1}$$

where the z dependence of E_ϕ has been neglected. We may express E_ϕ in terms of r_0, r_L, and ϕ through the following geometrical relations (see Fig. 1):

$$\begin{aligned} r&=(r_0^2+r_L^2-2r_0r_L\cos\phi)^{1/2}\ , \\ \cos\alpha&=[r_L+r_0\cos(\pi-\phi)]/r \\ &=(r_L-r_0\cos\phi)/(r_0^2+r_L^2-2r_0r_L\cos\phi)^{1/2}. \end{aligned}$$

Thus, we have

$$\begin{aligned} E_\phi&=E_{\theta 0}J_1[k_n(r_0^2+r_L^2-2r_0r_L\cos\phi)^{1/2}] \\ &\times(r_L-r_0\cos\phi)\,(r_0^2+r_L^2-2r_0r_L\cos\phi)^{-1/2} \\ &=-E_{\theta 0}k_n^{-1}\frac{\partial}{\partial r_L}J_0[k_n(r_0^2+r_L^2-2r_0r_L\cos\phi)^{1/2}]\ . \end{aligned} \tag{B2}$$

Expanding E_ϕ in terms of the sinusoidal harmonics of ϕ and noting that E_ϕ is an even function of ϕ, we obtain

$$E_\phi=\sum_{s=0}^{\infty}E_{\rm eff}^s\cos s\phi\ , \tag{B3}$$

where

$$\begin{aligned} E_{\rm eff}^s&=\frac{\Theta}{\pi}\int_0^{\pi}d\phi\,E_\phi\cos s\phi \\ &=-\Theta E_{\theta 0}(k_n\pi)^{-1} \\ &\times\frac{\partial}{\partial r_L}\int_0^{\pi}d\phi\,J_0[k_n(r_0^2+r_L^2-2r_0r_L\cos\phi)^{1/2}]\ , \end{aligned} \tag{B4}$$

$$\Theta=\begin{cases}1, & s=0,\\ 2, & s\neq 0\ .\end{cases}$$

Using tabulated integral formulas,[13] we obtain from Eq. (B4),

$$\begin{aligned} E_{\rm eff}^s&=-\Theta E_{\theta 0}J_s(k_nr_0)J_s'(k_nr_L) \\ &=-\Theta E_{\theta 0}H_s^{1/2}(k_nr_0,k_nr_L)\ . \end{aligned} \tag{B5}$$

[1] V. A. Flyagin, A. V. Gaponov, M. I. Petelin, and V. K. Yulpaten, IEEE Trans. Microwave Theory Tech. 25, 514 (1977), and references therein.

[2] J. L. Hirshfield and V.L. Granatstein, IEEE Trans. Microwave Theory Tech. 25, 522 (1977), and references therein.

[3] A. M. Kalmykov, N. Ya. Kotsarenko, and S. V. Koshevaya, Izv. Vyssh. Uchebn. Zaved. Raz. Radioelektron. 18, 93 (1975).

[4] E. O. Kane, J. Phys. Chem. Solids 1, 249 (1957).

[5] J. M. Ziman, *Principles of the Theory of Solids* (Cambridge U.P., London, 1964), p. 147.

[6] B. Lax, *Quantum Electronics* (Columbia U.P., New York, 1968), p. 248.

[7] H. J. Fossum and B. Ancker-Johnson, Phys. Rev. B 8, 2850 (1973).

[8] E. Ott and W. M. Manheimer, IEEE Trans. Plasma Sci. 3, 1 (1975).

[9] K. R. Chu, Naval Research Laboratory Memorandum Report (unpublished); Phys. Fluids (to be published).

[10] J. Gornik, T. Y. Chang, T. J. Bridges, V. T. Nguyen, J. D. McGee, and W. Muller, Phys. Rev. Lett. 40, 1151 (1978).

[11] D. E. Baldwin, J. B. Bernstein, and M. P. H. Weenik, in *Advances in Physics* (Interscience, New York, 1969), Vol. 3, p. 1.

[12] P. L. Bhatnagar, E. P. Gross, and M. Krook, Phys. Rev. 94, 511 (1954).

[13] M. Abramowitz and I. A. Stegun, *Handbook of Mathematical Functions* (Dover, New York, 1965), p. 363.

[14] S. M. Sze, *Physics of Semiconductor Devices* (Wiley, New York, 1969), p. 200.